Lateral Standing Spin Waves in Permalloy Antidot Arrays

G. Mankey – University of Alabama

et al.

Citation of published version:

Yu, C., et al. (2004): Lateral Standing Spin Waves in Permalloy Antidot Arrays. *Journal of Applied Physics*, 95(11). DOI: https://doi.org/10.1063/1.1687554

Lateral standing spin waves in permalloy antidot arrays

Cite as: Journal of Applied Physics **95**, 6648 (2004); https://doi.org/10.1063/1.1687554
Published Online: 25 May 2004

Chengtao Yu, Michael J. Pechan, Wesley A. Burgei, and Gary J. Mankey

Lateral standing spin waves in permalloy antidot arrays

Chengtao Yu, Michael J. Pechan, and Wesley A. Burgei
Department of Physics, Miami University, Oxford, Ohio 45056

Gary J. Mankey
The Center for Materials for Information Technology and Department of Physics and Astronomy, University of Alabama, Tuscaloosa, Alabama 35487

(Presented on 6 January 2004)

Spin wave modes in permalloy antidot arrays have been investigated with ferromagnetic resonance at 9.7 GHz. In contrast to a quadratic dispersion expected for exchange standing spin waves, nearly linear relationship exists between the resonance field and mode index, and it can be approximately described by the dipole-dipole and exchange theory. Time-dependent micromagnetic simulations show that the spin wave modes are a result of lateral confinement from the vacant holes. Furthermore, the simulations visually reveal the existence of localized spin waves due to localized boundary conditions in antidots arrays. © *2004 American Institute of Physics.*
[DOI: 10.1063/1.1687554]

I. INTRODUCTION

Dynamic properties of magnetic nanostructures are drawing increasing attention[1–5] as information technologists strive to increase the storage density and data throughput. One of the interesting dynamic phenomena is the spin wave excitation, which arises as a result of quantization in small structures when the structure dimensions become comparable to the wavelength of the spin waves. Spin wave modes have been observed in magnetic dots[1,2,4] and wires arrays[1,3] with Brillouin light scattering and are generally recognized as various dipole-dominant modes due to lateral confinement. However, very few ferromagnetic resonance (FMR) experiments have been conducted[6] on such nanomagnets, though FMR is a powerful tool in investigating spin wave spectra.[7] In this study, we present a detailed FMR investigation on the spin wave excitation in permalloy antidot arrays[8] and show that the spin wave spectra, which carry a linear dispersion can be approximately described according to a dipolar-exchange theory.[9] Furthermore, time-resolved micromagnetic simulations suggest these spin wave excitations are localized, with certain modes arising from well-defined positions within the antidot lattice.

II. EXPERIMENT

Magnetic permalloy polycrystalline films 40 nm thick were deposited onto native-oxide Si (001) substrates at a rate of ~ 1 Å/s by dc-magnetron sputtering. Utilizing premade masks, photolithography, and ion milling, magnetic antidot arrays (1.5 μm diameter holes in a continuous media) were prepared. The three samples presented in this report are rectangular arrays with center-to-center lattice parameter fixed at 3 μm in one direction and 4, 5, and 7 μm, respectively, in the orthogonal direction. The FMR measurements were carried out at 9.7 GHz with the magnetic field applied perpendicular to the plane of the film. Dynamic micromagnetic calculation of the magnetization precession of the antidot arrays were performed with the object oriented micromagnetic framework (OOMMF) software.[10]

III. RESULTS

Figure 1 shows the ferromagnetic resonance spectra measured for different antidot arrays along with the unpatterned sheet film. As seen, except for the sheet film [Fig. 1(a)], where a single uniform mode described by the Kittel formula [see Eq. (2)] occurs around 12.9 kOe, spin wave manifolds are observed on the low field side of the uniform mode for all samples. Note that the separation between adjacent spin wave peaks increases with the increase of the hole density, or decrease of the long axis of the rectangular

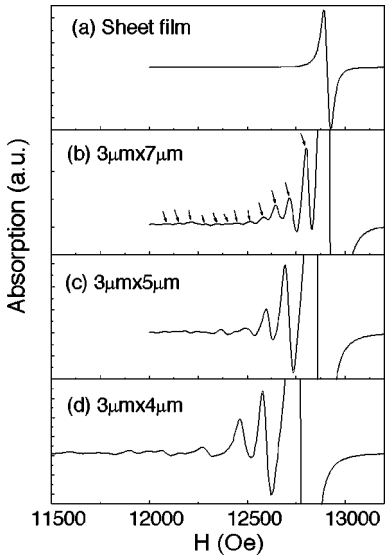

FIG. 1. FMR spectra in a perpendicular configuration (H normal to the film plane) for a permalloy sheet film (a), and antidots arrays (b)–(d). Arrows in (b) indicate positions of spin wave resonances and are indexed sequentially from high to low field.

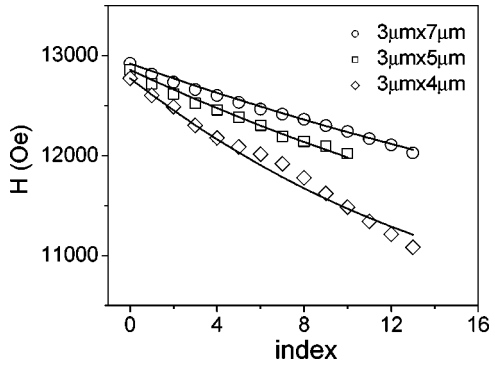

FIG. 2. Resonance fields of spin wave modes as a function of index number for the three antidot arrays. The solid lines are theoretical fittings from the Arias and Mills dipole-exchange theory.

antidot. This indicates that the spin wave vectors, expressed as $k=n\pi/L$ (L is the characteristic length along the wave direction), scale with the antidots mesh size. In other words, the observed spin wave modes are the quantized results of spin waves under the lateral boundary conditions set by the holes. The shifts of the whole spectrum toward lower fields as the hole mesh changes from $3\times7\ \mu\mathrm{m}^2$ to $3\times4\ \mu\mathrm{m}^2$ are related to the hole density, which directly affects the perpendicular demagnetization factor, $4\pi\mathrm{M}$ [see Eq. (2)], as discussed in a previous paper.[11]

The resonance field as a function of the index number of the spin wave modes is given in Fig. 2, where the spin wave modes are labeled with both even and odd integrals without considering selection rules. Interestingly, approximate linear dispersions are observed in contrast to the classical quadratic dispersion expected for perpendicular standing spin waves due to exchange.[12] This suggests dipolar coupling, arising either from surface or volume charge in a saturation state, may govern the spin wave mechanism. By considering both dipole-dipole and exchange coupling among spins, there have been several theoretical treatments. Herein we utilize Arias and Mills[9] model to interpret the experimental data. The condition of ultrathin film described in this scheme, where perpendicular standing spin wave frequencies are shifted well above the uniform FMR frequency by exchange is met in our 40 nm thick films, as even for the first order, perpendicular standing spin wave mode would be observed several kilo-oersteds away from the uniform peak. With applied field normal to the film plane, the dispersion relation for a transverse in-plane spin wave is expressed as

$$\left(\frac{\omega(k_\parallel)}{\gamma}\right)^2=(H-4\pi M)^2+2(H-4\pi M)\left(\pi M k_\parallel d+\frac{2A}{M}k_\parallel^2\right), \tag{1}$$

where γ is the gyromagnetic ratio, H is the external field, M is the saturation magnetization, d is the film thickness, and A is the exchange stiffness constant. $k_\parallel^2=k_x^2+k_y^2$ is the in-plane spin wave vector determined by the boundary condition. When the wave vector $k_\parallel=0$, the dispersion reduces to the well-known Kittel equation[12] [realized in Fig. 1(a)]

$$\frac{\omega_0}{\gamma}=H-4\pi M. \tag{2}$$

For simplicity, we assume $k_\parallel=n\pi/L$, where L is a lateral length parameter determined by the boundary condition or hole separation, and n is an integer. Given $f=9.7$ GHz, $\gamma=1.91\times10^7\ \mathrm{sec}^{-1}\,\mathrm{G}^{-1}$, $d=40$ nm, $A=1\times10^{-6}$ erg/cm for permalloy film, M extracted from the uniform resonance peak, and L as a fitting parameter, the experimental data are modeled with the above mentioned spin wave dispersion equation and plotted as solid lines in Fig. 2. As seen, the best fittings for the three rectangular samples $3\times4\ \mu\mathrm{m}^2$, $3\times5\ \mu\mathrm{m}^2$, and $3\times7\ \mu\mathrm{m}^2$ give lateral length parameters about 1.8, 3, and 4 μm, respectively. We have also calculated the characteristic length according to a more sophistical treatment of spin wave dispersion by Kalinikos[13] and the outcome is comparable. The fact that these characteristic lengths are so close to the hole separations indicates that the observed spin wave modes have their origin in the lateral confinement from the vacant hole arrays. The confinement is indeed visualized from the time-resolved magnetic domains as shown in the following.

Time-dependent micromagnetic simulations have been carried out to help visualize the spin wave formation and propagation. The calculations are based on Landau-Lifschitz-Gilbert formula on a mask with four holes. Initially, all spins are set parallel to each other and have a small deviation ($\sim1°$) from the external dc field, which is normal to the film plane and has the same magnitude as the uniform resonance field in the FMR experiment (≈13 kOe). With a small damping factor (~0.0005), the spins start to precess around the field direction according to Landau-Lifschitz motion equation. At first, all spins precess uniformly, but with elapsing time, magnetic in-plane phase domains emerge and evolve into wave patterns, manifesting the existence of in-plane spin wave excitations. Shown in Fig. 3(a) is a snapshot of the spatial distribution of y-component magnetization (M_y), which somehow illustrates the time-dependent spin waves in real space. Lateral wave patterns are clearly observed, which are direct evidence of spin wave propagation. The wave patterns change with time, yet the waves themselves are confined by the boundaries of the hole edges, which sets the in-plane wave vector to quantized values, $k_\parallel=n\pi/L$. Although the entire image may be made up of many waves (e.g., different L and n) interacting as they traverse the media, it is evident that localized modes exist in certain regions due to different boundary restrictions. For example, the parts between the nearest holes see different boundary restriction than the diagonal central part of the hole mesh. It is noteworthy that such localization of spin waves has a different source than the localized ferromagnetic resonance observed in antidots at 35 GHz in a previous paper,[11] and the localized edge modes of spin waves observed in magnetic wires in a BWVMS (backward volume magnetostatic spin wave) geometry due to localized demagnetization fields,[14] whereas in this case the localizations are caused by the localized boundary conditions.

The inset of Fig. 3(b) shows the behavior of the total magnetization M_y as a function of simulation time, from

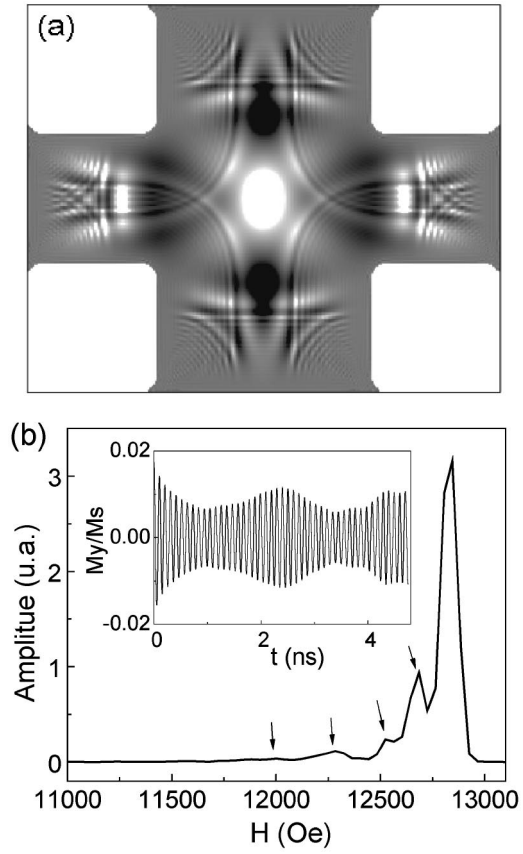

FIG. 3. Time-dependent micromagnetic simulations of the antidot arrays ($3\times4\ \mu m^2$). (a) Snapshot of the spatial magnetization M_y distribution. (b) Simulated FMR spectra converted from the frequency spectra (not shown). The arrows indicate the spin wave modes. The inset shows M_y as a function of simulation time. (Note $M_z \approx M_{sat}$ is normal to the page.)

which the spin wave frequency spectrum can be obtained via Fourier transform. Upon converting from a frequency spectrum at constant field to a field spectrum at constant frequency, Fig. 3(b) shows the resultant FMR spectra obtained from the simulation. As seen, beside the main uniform mode, higher order spin wave modes appear on the low field side as anticipated. The separation between the uniform and first satellite peak is about 144 Oe, which is reasonably close to the experimental observation (170 Oe), especially considering the boundary effects arising from the finite size of the simulated sample. It should be mentioned that the spectrum obtained in this simulation averages out detailed information on the localized spin waves, because the total magnetization is used in the Fourier transform. It should also be pointed out that such localization was also ''averaged over'' in our application of Arias and Mills model, which yielded spin waves from an average length, whereas in fact several sets of spin waves with different $k_{\|}$ might be excited simultaneously. In the future, it would be interesting to study the localized spin wave modes experimentally by utilizing nanoscale ferromagnetic resonance techniques or time-resolved Kerr microscopy.[14]

In conclusion, lateral spin wave modes have been experimentally observed in antidot arrays with FMR technique, and as shown by dynamic micromagnetic simulations, the spin waves are confined by the hole boundaries and localized excitation may exist. The spin wave dispersion can be approximately interpreted in terms of dipole-exchange spin wave excitation in a thin film limit.

ACKNOWLEDGMENT

This work was supported by U.S. DOE Grant Nos. DE-FG02-86ER45281 (MU) and NSF DMR-0213985 (UA).

[1] J. Jorzick *et al.*, J. Appl. Phys. **89**, 7091 (2001).
[2] S. Jung, B. Watkins, L. Delong, J. B. Ketterson, and V. Chandrasekhar, Phys. Rev. B **66**, 132401 (2002).
[3] Z. K. Wang *et al.*, Phys. Rev. Lett. **89**, 027201 (2002).
[4] G. Gubbiotti, G. Carlotti, R. Zivieri, F. Nizzoli, T. Okuno, and T. Shinjo, J. Appl. Phys. **93**, 7607 (2003).
[5] V. Novosad, M. Grimsditch, K. Yu. Guslienko, P. Vavassori, Y. Otani, and S. D. Bader, Phys. Rev. B **66**, 052407 (2002).
[6] Y. Zhai, J. Shi, X. Y. Zhang, L. Shi, Y. X. Xu, H. b. Huang, Z. H. Lu, and H. R. Zhai, J. Phys.: Condens. Matter **14**, 7865 (2002).
[7] For example, M. H. Seavey, Jr., and P. E. Tannenwald, J. Appl. Phys. **30**, 227S (1959).
[8] C. T. Yu, H. Jiang, L. Shen, P. J. Flanders, and G. J. Mankey, J. Appl. Phys. **87**, 6322 (2000).
[9] R. Arias and D. L. Mills, Phys. Rev. B **60**, 7395 (1999).
[10] M. J. Donahue and D. G. Porter, http://math.nist.gov/oommf
[11] C. Yu, M. J. Pechan, and G. J. Mankey, Appl. Phys. Lett. **83**, 3948 (2003).
[12] C. Kittel, Phys. Rev. **110**, 1295 (1958).
[13] B. B. Kalinikos and A. N. Slavin, J. Phys. C **19**, 7013 (1986).
[14] J. P. Park, P. Eames, D. M. Engebretson, J. Berezovsky, and P. A. Crowell, Phys. Rev. Lett. **89**, 277201 (2002).